



Research paper

Conceptual design of a sorption-based cryochain for the ETpathfinder

A. Xhahi^{a,b,*}, H.J. Holland^a, H.J. Bulten^b, H.J.M. ter Brake^a^a University of Twente, Faculty Science and Technology, P.O. Box 217, Enschede, 7500AE, the Netherlands^b NWO-i Nikhef, P.O. Box 41882, Amsterdam, 1009DB, the Netherlands

ARTICLE INFO

Keywords:

Sorption cooler
 Gravitational wave detection
 Cryochain
 Vibration-free cooling
 Cryogenic optics

ABSTRACT

Next-generation gravitational wave detectors, including the Einstein Telescope [1] [2], aim to achieve amplitude-spectral-density strain sensitivities on the order 10^{-24} m/ $\sqrt{\text{Hz}}$ [3]. In the low-frequency band such sensitivities can only be obtained when thermal noise, mainly stemming from the mirror coating, is reduced by employing cryogenic cooling techniques for the mirrors. The optical surface of the mirror should not vibrate with strain noise amplitude spectral densities above 10^{-20} m/ $\sqrt{\text{Hz}}$ for the cryogenic mirrors in the Einstein Telescope [3]. The ETpathfinder research facility [4] [5], aims to facilitate the development and testing of critical new technologies required for the design and operation of future gravitational wave detectors. A key enabling technology for the design and operation of such advanced interferometers is the cryogenic system that cools the main optics to a temperature of approximately 10 K. Given the stringent requirements on vibrational noise for these optics, the cryogenic cooling under continuous operation should be essentially vibration free. Joule-Thomson cryocoolers using sorption compressors are known to generate an absolute minimum of vibrational noise during operation. We propose a modular cryochain design comprised of a system of sorption compressors and Joule-Thomson cold stages fitting the ETpathfinder project requirements. In this paper, we present the conceptual design of the cooler chain that is based on a parallel cascade arrangement of a 40 K neon stage, a 15 K hydrogen stage and a 8 K helium stage. The operating parameters of the sorption-based cooler chain are selected via a hybrid modeling workflow, aiming to optimize performance and other design considerations within an envelope of acceptable design parameters.

1. Introduction

The Einstein Telescope (ET) is a future European Gravitational Wave (GW) Observatory that is included in the 2021 road-map of the European Strategy Forum on Research Infrastructures (ESFRI) [6]. ET is envisioned to be built underground so as to reduce seismic noise along with other environmental perturbations [1]. The observatory targets to detect a wide range of GW phenomena with greater sensitivity and in a larger frequency band than the current state of the art operational (2G) GW observatories around the world, such as LIGO [7], VIRGO [8] and KARGA [9]. The improved sensitivity in the measurements will be enabled by the utilization of new generation detectors [10]. Relative changes of less than 10^{-21} meters are expected to be measured by the ET interferometers [2] [3]. In order to achieve precision measurement capabilities of this caliber a number of new enabling technologies need to be developed. Critical technologies and techniques required for the realization of ET include a sophisticated suspension system, low-noise

mirror coatings, vibration-free cryogenic cooling and installation of a large underground ultra-high vacuum facility [10] [11]. Prior to the industrialization and construction of such a massive project the aforementioned technologies need to be developed, tested and qualified. For this purpose a novel research facility, named ETpathfinder, is currently being constructed at the University of Maastricht [10]. The improvement in the measurement capabilities is to a large extent attributed to operating the detectors at a cryogenic temperature of about 10 K [2] [12]. Cryogenic operation substantially reduces the noise caused by thermal activity on the coating of the mirrors [12] [4]. Therefore, the cryogenic cooling of the optical system is a key design aspect in the sensitivity enhancement of the 3G GW detectors, especially at low frequencies. The baseline cooling system of the ETpathfinder starts with a liquid nitrogen bath that cools a thermal radiation shield, thus intercepting radiative heat loads from the 300 K external environment. To minimize the heat loads to the mirror we intend to have two more thermal shields inside the nitrogen-cooled shield, in order to further

* Corresponding author at: University of Twente, Faculty Science and Technology, P.O. Box 217, Enschede, 7500AE, the Netherlands.
 E-mail address: a.xhahi@utwente.nl (A. Xhahi).

Nomenclature

Latin letters

c_p	Specific heat capacity at constant pressure	$\text{J kg}^{-1} \text{K}^{-1}$
e	Specific exergy	J kg^{-1}
ϵ	Effectiveness of heat exchange	%
g	Specific Gibbs free energy	J kg^{-1}
h	Specific enthalpy	J kg^{-1}
L	Length of sorption cell	mm
m	Mass	kg
\dot{m}	Mass flow rate	kg s^{-1}
N_{cell}	Number of the compressor cell	-
P	Pressure	Pa
\dot{Q}	Heat-flow rate (Power)	W
Q	Volumetric heat-flow rate	W m^{-3}
r	Radius	mm
q	Specific energy	J kg^{-1}
t	Time	s
T	Temperature	K
x	Amount of gas normalized to the adsorbent mass	kg kg^{-1}

Greek letters

Δ	Difference	-
λ	Thermal conductivity	$\text{W m}^{-1} \text{K}^{-1}$
ρ	Density	kg m^{-3}

Subscripts

<i>ads</i>	Adsorbed phase
<i>c</i>	Cooling
<i>carb</i>	Adsorbent (activated carbon)
<i>cell</i>	Sorption cell
<i>cont</i>	Container

<i>cycle</i>	Sorption compressor cycle
<i>g</i>	Gaseous phase
<i>H</i>	High temperature/pressure
<i>He</i>	Helium
H_2	Hydrogen
<i>ht</i>	Heater
<i>in</i>	Input
<i>ins</i>	Insulation/isolator
<i>JTCS</i>	Joule-Thomson cold stage
<i>L</i>	Low temperature/pressure
<i>Ne</i>	Neon
<i>opt</i>	Optimum
<i>Prec</i>	Pre-cooling
<i>SC</i>	Sorption compressor
<i>sink</i>	Related to the thermal sink
<i>sorp.</i>	Related to the adsorption process (heat)
<i>tot</i>	Total

Abbreviations

<i>2G</i>	Second generation
<i>3G</i>	Third generation
<i>CFHX</i>	Counter flow heat exchanger
<i>CHX</i>	Cold-tip heat exchanger
<i>COP</i>	Coefficient of performance
<i>ET</i>	Einstein Telescope
<i>GW</i>	Gravitational wave
<i>I/F</i>	Interface
<i>JT</i>	Joule-Thomson
<i>JTR</i>	Joule-Thomson restriction
LN_2	Liquid nitrogen
<i>UT</i>	University of Twente

reduce the radiative heat flow. Moreover, thermal anchoring can be applied so as to reduce the conductive heat loads as well. These inner two shields and the cold finger need to be actively cooled in continuous operation to temperatures well below that of the liquid-nitrogen bath. The operating temperatures and cooling loads are summarized in Table 1 and further explained in section 2.2. The main requirement is that the cooling system should not generate vibrations at the cold finger exceeding the level caused by seismic excitation of the ground. At the ETpathfinder site, seismic excitation with an amplitude spectral density of $4 \text{ nm}/\sqrt{\text{Hz}}$ has been measured in the frequency band 2 – 10 Hz, corresponding to about 30 nm peak-to-peak displacement [5]. Considering that ET itself will be installed underground, its seismic levels are expected to even be one order of magnitude lower [11].

Consequently, a cooling system is sought that can provide adequate cooling at three temperature levels with negligible vibration generated at the cold finger. Traditional cryogenic coolers, such as Stirling cryocoolers, Pulse-Tubes, mechanical Joule-Thomson (JT) cryocoolers and Gifford-McMahon (GM) coolers, are commonly utilized for ground-based scientific instrumentation. Despite their widespread use, these cooling systems incorporate mechanical compressors, which invariably produce and consequently transfer vibrational noise to the cryogenic payload [13]. Thus, these cooling systems require active and sophisticated attenuation mechanisms to mitigate the transmission of vibration to the cryogenic payload. Even with these measures, it remains highly unlikely that the vibration requirement level for GW detectors—both in terms of magnitude and frequency—can be feasibly met using mechanical coolers [13]. A promising alternative that is known for its inherit vibration-free operation, is the use of sorption-based Joule-Thomson (JT) coolers. JT cold stages can be operated with sorption compressors that consist of one or more sorption cells. Where each cell houses a con-

Table 1
ETpathfinder cryostat cold tip temperature and cooling loads specifications for the baseline design.

Thermal Compartment	Cold Tip Temperature (K)	Cooling Load (W)
Radiation shield: intermediate ^a	40	2.5
Radiation shield: inner ^a	15	0.5
Cold finger	8	0.05

^a The shield qualitative characterization as intermediate is defined in accordance with the ETpathfinder thermal environment description in section 2.2.

tainer that is filled with an adsorbent material such as activated carbon. Sorption compressors are thermally driven, and by controlling the gas-flow direction with passive valves, a nearly continuous flow of gas can be maintained through a JT cold stage. Apart from the passive valves, these coolers have no moving parts and hence deliver highly reliable vibration-free operation with a long lifetime [14] [15] [16] [17].

A schematic of an archetypal sorption-based JT cryocooler is depicted in Fig. 1. It comprises a compressor cell, two buffer volumes, and a pair of passive valves. The gas flows from a low-pressure buffer to a high-pressure one via the sorption cell, driven by two main processes involving cyclic heating and cooling of the adsorbent within the cell. Once in the high-pressure buffer, the gas then passes through a counter-flow heat exchanger (CFHX) to reach the JT flow restriction. At this point, the gas undergoes an isenthalpic expansion to the low-pressure value, leading to a temperature drop in the gas, and potentially, its liquefaction. The expanded fluid absorbs heat from its surroundings and returns through the CFHX, exchanging heat with the incoming high-pressure flow. At the University of Twente (UT) a great deal of research has been dedicated to the thermodynamic operation and op-

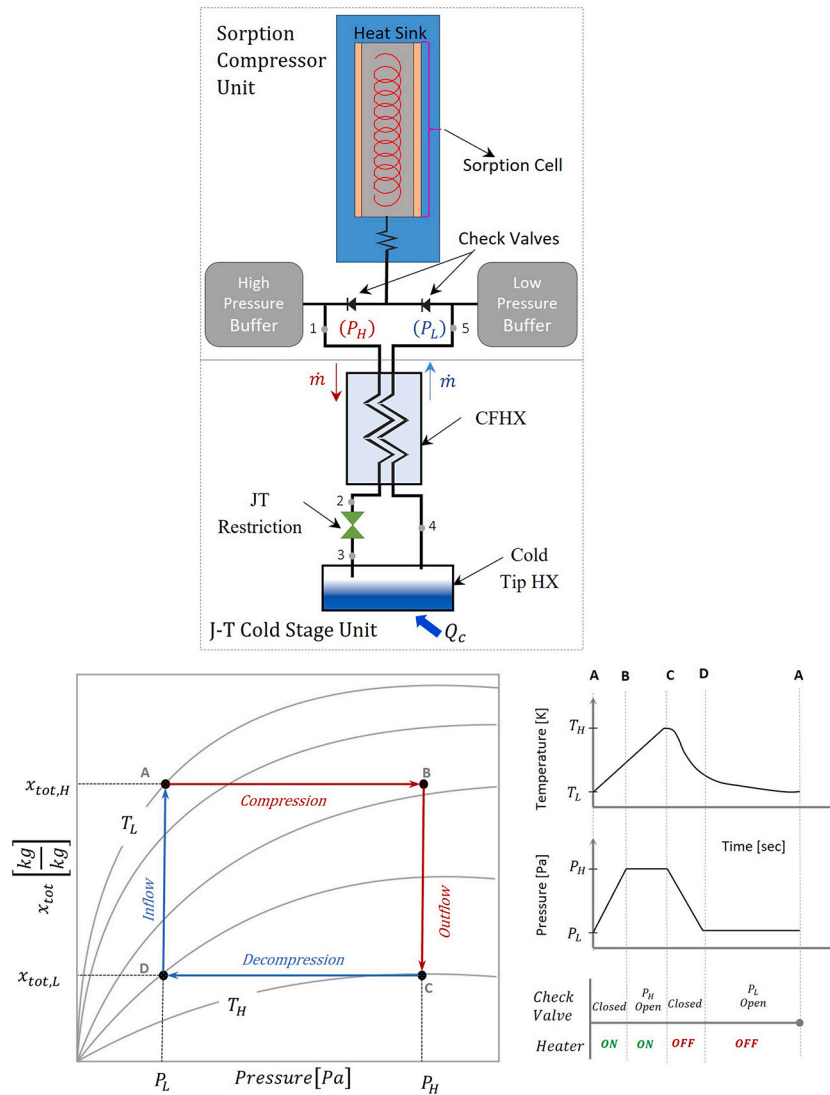


Fig. 1. Schematic depiction of a sorption-based JT cooler (top) and corresponding sorption cycle (bottom). In the initial state A the sorption compressor is heated. Gas is desorbed and thus pressure increases in the compressor cell. Upon reaching high pressure P_H (state B), the high-pressure valve opens, allowing gas to flow out of the cell. The heating continues until T_H is reached in the cell (state C). Then, heating is stopped and the temperature and pressure in the cell start to drop. As a result, the high-pressure check valve closes. Because of the thermal contact with the heat sink the cell further cools and the pressure in the cell reduces until the low pressure is reached (P_L). At this point, the low-pressure check valve opens (state D) and working gas starts flowing into the compressor to get adsorbed while cooling in the cell continues. Once the low temperature (T_L) is reached the sorption cycle restarts in state A.

timization of sorption-based cryocoolers for different applications [14] [18]. The requirements of ETpathfinder listed in Table 1 resemble those of the METIS instrument in E-ELT for which the Energy Material & Systems group at the University of Twente has developed a sorption-based cooler chain [19]. Therefore, this METIS cooler was taken as a starting point in the design of the ETpathfinder cooler chain. This paper presents the conceptual design of the ETpathfinder sorption-based cooler chain. The preliminary design process and analysis is discussed in section 2, whereas the resulting baseline cryochain design is presented in section 3. The paper closes with conclusions and projected research in section 4.

2. Development of the ETpathfinder cryochain conceptual design

This section discusses the development process of the conceptual design of the ETpathfinder cryochain. First, a generic explanation of the ETpathfinder cryogenic systems configuration is given in section 2.1 followed by a more detailed description of the cryogenic payload thermal environment (cryostat) in section 2.2; the sorption cryochain architec-

ture and the sorption compressor design are presented in sections 2.3 and 2.4, respectively; section 2.5 gives a detailed description of the modeling approach and model validation; assumptions and design margins are specified before discussing the process for selecting the operating parameters of the respective cooler stages.

2.1. ETpathfinder cryogenic systems configuration

At stable operating conditions during measuring mode of below 20 K (Phase 1.b) [2], the sorption cryochain will be the principle cryogenic system cooling the interferometer mirrors. In addition to the sorption cooler chain an auxiliary cooling system will be installed for cooling down the entire system from room temperature to cryogenic temperatures. A powerful liquid nitrogen cooling system will have the capacity to evacuate hundreds of Watts during the cool-down phase. The LN_2 cooling system will also provide the cooling of the LN_2 shield during operation (measurement phase) of the interferometer via a vessel (filled with LN_2) mounted at the bottom of that radiation shield (further details are offered in section 2.2). Furthermore, the system will be cooled

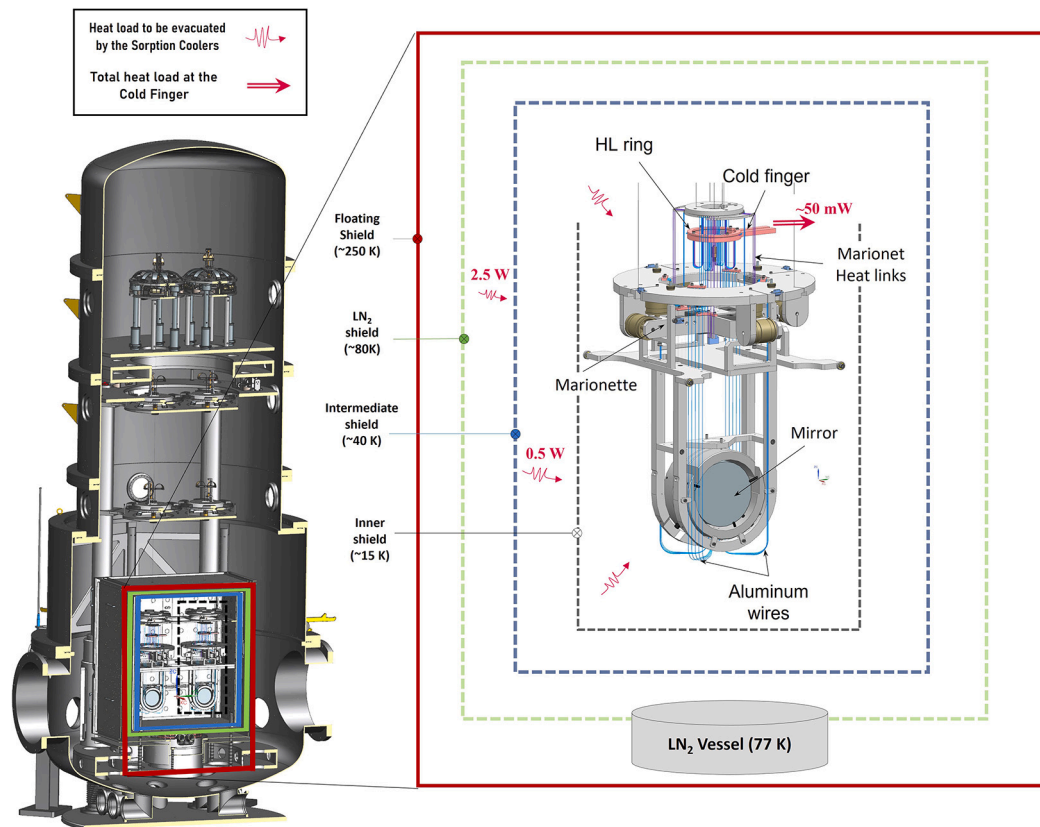


Fig. 2. Left: cross section of the Mirror vacuum tower; Right: schematic of the ETPATHFINDER's payload thermal environment (cryogenic enclosure).

down by a convective helium gas loop that is cooled by a mechanical cooler. Once the targeted operating temperature of around 10 K is reached, this loop will be switched off and the sorption cooler will take over.

2.2. Cryogenic payload thermal environment (mirror's cryostat)

As discussed above and also shown in Fig. 2, the thermal environment of the cryogenic payload (mirrors, marionettes, etc.) is formed by a nested arrangement of thermal shields. These shields minimize the heat load on the cryogenic payload. It is worth mentioning that extremely high vacuum is required inside the tower to prevent residual gas depositing on the cold mirrors and hence multi-layer insulation (MLI) cannot be applied (for out-gassing reasons). Each thermal shield in ETPATHFINDER, except the final 15 K shield, is made of a double-walled aluminum structure with staggered holes for pumping [2]. Fig. 2 also provides a visual representation of the temperatures and geometry associated with the thermal shields. The 15 K shield is open on the top side, since accommodating the mirror suspension would make adding a top plate overly complex. The operating steady-state temperature of the outer floating shield is calculated to be about 250 K whereas that of the LN₂ shield, which is cooled at the bottom by the LN₂ vessel, will be at 80–90 K [2]. The LN₂ vessel in the mirror tower operates at atmospheric pressure (1 bar) resulting in an operating temperature of ~77 K. Furthermore, the intermediate shield is assumed to be at 40 K with a heat load of 2.5 W (dominated by radiation), while the innermost shield is at 15 K with an anticipated heat load of 0.5 W. The primary function of the thermal shields is to reduce the radiative heat loads. As a secondary function these shields aim to provide thermal anchoring of wiring and other support structures, resulting in reduced conductive heat loads. In stationary operation, the total heat load on the cryogenic payload is expected to be 50 mW. The temperature stability of the cold tip is not explicitly specified as a requirement. Any fluctuations in the

cold tip's temperature are substantially damped by the thermal resistances and thermal mass in the connections between the cold tip and the mirror (as depicted in Fig. 2). Nevertheless, if there is a need for more precise thermal control of the cold tip, we will be able to stabilize the tip temperature to millikelvin level [16].

2.3. Sorption cryochain architecture

The baseline cryochain architecture we developed for the ETPATHFINDER cryostat is illustrated in Fig. 3. It is based on a modular parallel arrangement of three sorption cooler stages. Due to the operating temperature specifications, the selection of working gases is limited. Helium is the only option for the 8 K cooling stage. Hydrogen is chosen as the working fluid for pre-cooling the helium stage at 15 K and also provides cooling for the inner radiation shield. Neon is the sole viable choice for the 40 K cooling requirement of the intermediate radiative shield. Furthermore, the neon stage supplies pre-cooling power for the hydrogen stage and the first pre-cooling step for the helium stage. To enable servicing and/or adapting the sorption compressor unit without breaking the main vacuum of the interferometer, the compressor unit will be placed in a separate vacuum chamber with the working-fluid lines connecting to the mirror vacuum tower. The sorption compressor unit is envisioned to be cooled via a dedicated LN₂ refrigeration loop at 70 K, corresponding to a sub-atmospheric operating pressure of 0.39 bar.

2.4. Sorption compressor design

The sorption compression cell design used in the dynamic model calculations of this work, is based on the switchless concept proposed and experimentally tested by Y. Wu et al. [20] [21]. Due to its inherent advantages of simplified manufacturing and operation, and having a compact form factor, this cell design avoids the practical complexities of a gas-gap heat switch design [20] [21]. Geometric features of the cell

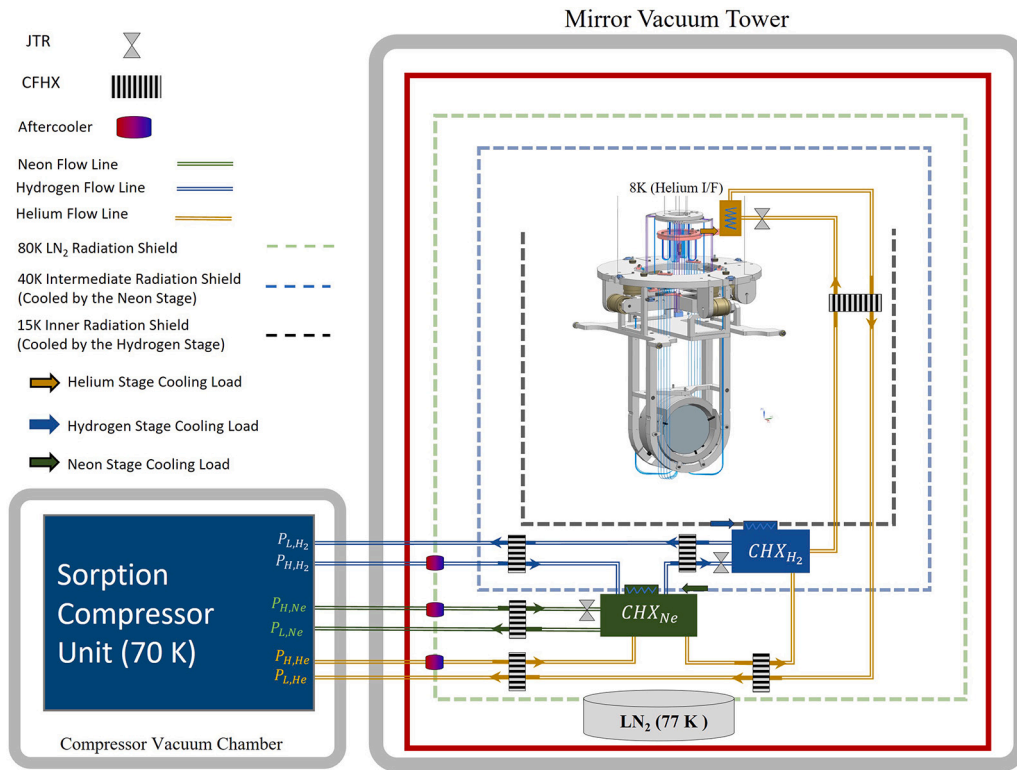
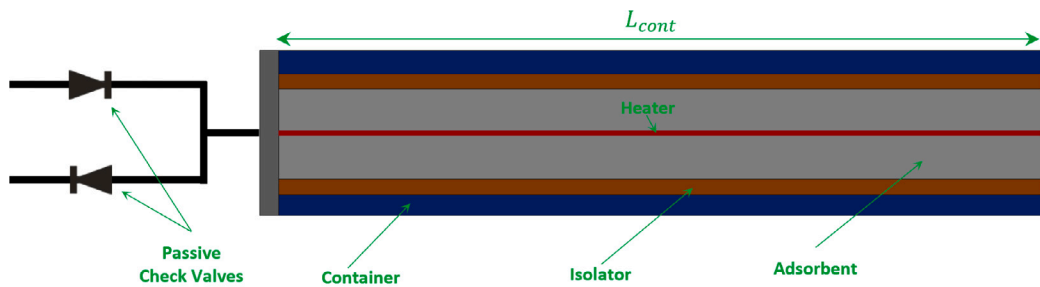
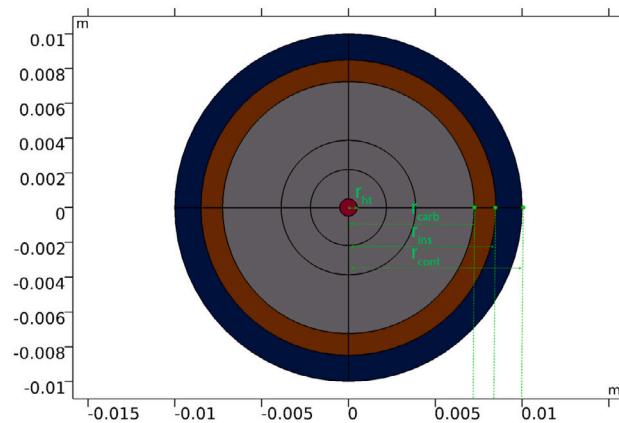


Fig. 3. Schematic of the proposed sorption-based cryochain architecture (inside the cryostat) depicting the envisioned thermal interfaces with the shields as well as the interlinked pre-cooling paths.



(a) The longitudinal cross section of the sorption cell design used in ETpathfinder cryochain; with single central heater (in red); adsorbent material (in dark grey); insulation layer (in orange) and the SS136L container wall (in dark blue).



(b) Radial cross section of sorption cell design. The axes represent the cell dimensions. Outer cell diameter is 20 mm

Fig. 4. Sorption compressor cell: cross section profiles.

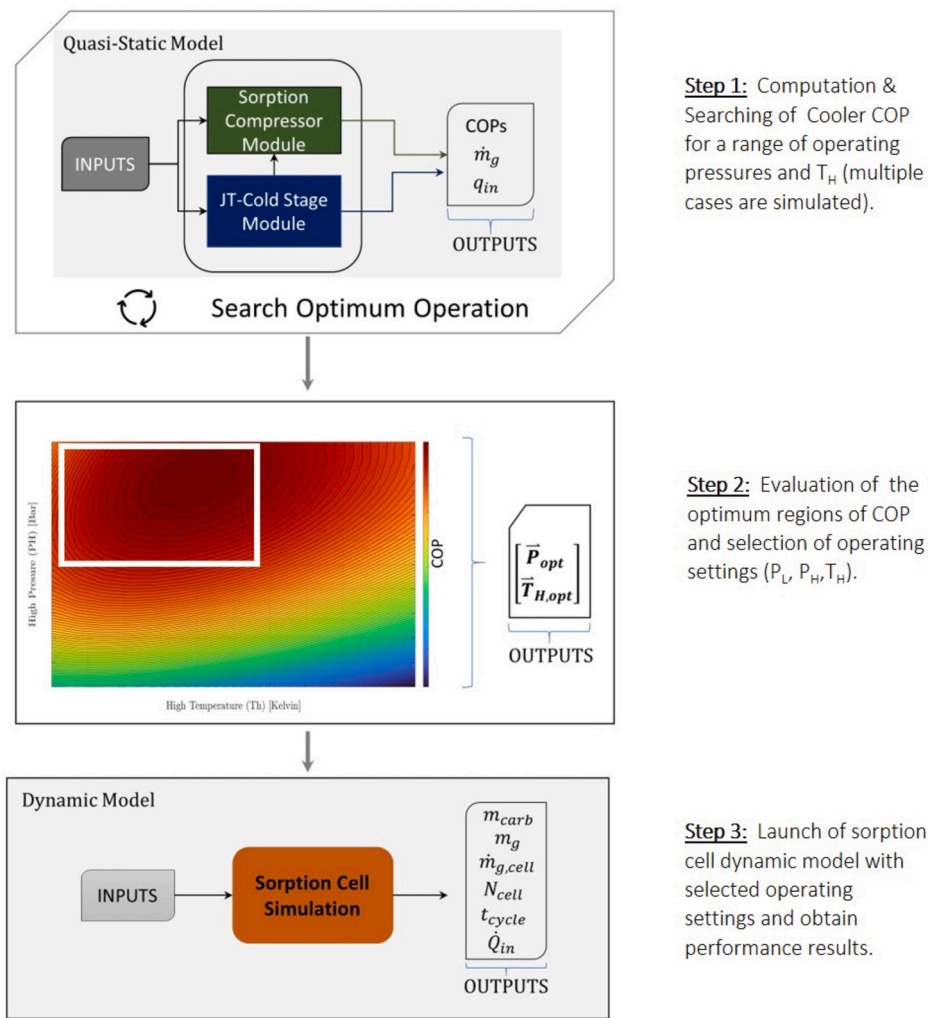


Fig. 5. ETpathfinder cryochain simulation workflow (optimization).

Table 2
Baseline dimensions and materials of the compressor cell design.

Parameter description	Symbol	Value	Unit	Material
Radius of the heater	r_{ht}	0.5	mm	SS-316L ^a
Radius of the adsorbent	r_{carb}	7.25	mm	Saran
Radius of the insulation	r_{ins}	8.5	mm	Kapton (Polyimide) ^a
Radius of the container	r_{cont}	10	mm	SS-316L ^a
Length of the cell	L_{cont}	500	mm	-

^a Material thermal properties were obtained from the NIST database [22].

design are visible in Fig. 4. A summary of the selected materials and cell dimensions which are used throughout the simulations are given in Table 2. The container wall thickness depends on the maximum internal pressure and on the cell placement inside the heat sink. In this design phase a container thickness of 1.5 mm is assumed. Each cell contains 90.4 grams of Saran activated-carbon.

2.5. Sorption cryochain modeling & validation

2.5.1. Modeling approach: sorption-based JT cooler

A hybrid modeling approach was developed for the preliminary design evaluation of the ETpathfinder sorption cryochain. More precisely, a quasi-static (thermodynamic) model was employed in conjunction with a dynamic (thermo-adsorption) model. The quasi-static model of the sorption cooler basically provides information about the thermodynamic performance (in terms of COP) and the mass flows that are

required to meet the cooling loads defined by the project specifications. However, since the quasi-static model does not provide any information about the evolution of temperature and pressure in time, it cannot evaluate the effect of cell dimensions nor determine the resulting required mass of the adsorbent material. Hence, a dynamic model was developed to simulate the dynamic behavior of the sorption compressor. Fig. 5 depicts the implemented simulation workflow, which can be divided into three major steps.

First, the quasi-static model is launched multiple times in an attempt to explore the operating design space of the sorption cooler. The parameters that are varied within this design space are the operating pressures (high and low pressures of the three stages, P_H and P_L) and the compressor high temperatures for the three stages (T_H). The other parameters (i.e. heat-sink temperature, working fluid & adsorbent, cooling loads, tip temperatures, isotherm data, CFHX efficiencies) are provided as input data and are fixed in the analysis. As an output of this first step a database is created of all the computed cases including the COP's of the cold stages, the required mass-flow rates, and the theoretically minimum required compressor input powers. The latter, minimum input power, accounts for the sensible heat of the adsorbent material and the heat of desorption. Parasitic terms such as the sensible heat of the container material are not included yet.

Second, we evaluate the simulated cases by generating performance contour graphs (see Fig. 5: Step 2). The search algorithm we used for the optimization of the operating settings (operating pressures and compressor high temperature) is based on a full factorial design approach

Table 3
Cryochain design margins.

Parameter	Value	Unit	Description
$\Delta T_{L,sink}$	1	K	Difference between heat sink temperature and lowest operating temperature inside the sorption cell (adsorbent)
ΔT_{Prec}	0.5	K	Difference in temperature between precooler and circulating fluid
ΔQ_{Prec}	+20	%	Margins in precooling loads
ϵ_{CFHX}	Helium [99.5, 99, 98.5] Hydrogen [98, 98] Neon [97]	%	Cold stage CFHXs efficiencies (the order of values in the brackets starts from coldest to warmest heat exchanger)

[23]. With this approach it was possible to efficiently and adequately explore the design space of the operating parameters, avoiding blind optimization decisions which can lead to premature system over-design. In the ETpathfinder project two design parameters have been identified to be of most interest at the system level, namely, the size of the cryo-chain (in terms of volume) and the required heat input (power). Under these constraints, the cooler's *COP* is the chosen parameter to be maximized in this optimization search. Therefore, the selection of the set of operating conditions for each stage is made on the basis of providing a satisfactory cooler *COP* performance with minimum required mass flow.

Third, we insert the selected optimized operating settings for each stage into the sorption cell dynamic model along with other input parameters (i.e. cell geometry, material properties, heating power). The dynamic model computes the cycle time, the required amount of adsorbent (activated carbon) needed to produce the required flow rate and the resulting number of compressor cells. Both models were developed in MATLAB® using REFPROP10® as a fluid library. The isotherm data are another important set of inputs to the model. The adsorption isotherm data for the three working fluids are derived from experiments performed at the University of Twente in previous sorption cooler projects [24].

2.5.2. Design margins, assumptions & idealizations

The design margin philosophy we applied to this conceptual design phase is presented in Table 3. Furthermore, the following assumptions and idealizations are used in our models:

1. In the dynamic model only heat transfer in the radial direction is considered (1D). Hence, temperature gradients only in that radial direction are accounted for;
2. A boundary heat-sink node at constant temperature (70 K) is set to be in contact with the outer surface of the compressor container;
3. Lumped capacitance formulation is used for the discretization of the nodes (isothermal regions);
4. The pressure in the cell is assumed to be uniform at all times (i.e. no pressure gradient across the adsorbent inside the cell);
5. The high pressure gas entering the cold stage is set at heat sink temperature of the cold stage (77 K);
6. During inflow and outflow phases the cell pressure is assumed to be constant: P_L and P_H , respectively;
7. There is no pressure drop in the system other than that across the JT restriction. Also, check valves do not impose any flow impedance;
8. All thermodynamic processes are ideal and quasi-static, except the CFHX's heat transfer (these CFHX's have efficiencies as specified in Table 3);
9. The only void volume in the compressor is that caused by the porosity of the adsorbent. Other void volume contributions are not included (such as volume in the flow tubes or check valves);

10. Thermal contact conductance at interfaces is assumed to be perfect. Thermal contact resistances (other than those specified in Table 3) are neglected;
11. The adsorption and desorption processes are assumed to respond instantaneously to changing parameters (such as temperature and pressure). This implies that the working fluid mass balance can be determined at any moment in time on the basis of temperature and pressure.

2.5.3. Step 1: quasi-static model

In the first step of the analysis, the quasi-static model treats the sorption compressor as a singular cell, setting aside considerations of physical dimensions and transient characteristics. Here the ideal formulation of the thermodynamic model is presented. Typically, the overall *COP* of the individual sorption cooler stage is determined as the product of the *COP* of the cold stage and the *COP* of the compressor.

$$COP_{Cooler} = COP_{SC} \cdot COP_{JTCS} \quad (1)$$

The Coefficient of Performance for the sorption compressor, denoted as COP_{SC} , is defined as the ratio of the specific exergy (e), representing the ideal work done to compress the working gas, to the input heat required per unit of adsorbent material. The exergy is calculated for each cycle of the process as the product of the net amount of gas desorbed (Δx_{net}) per mass of adsorbent material and the specific exergy per unit of gas [14]. Then, the compressor *COP* follows as:

$$COP_{SC} = \frac{e}{(q_{in}/\Delta x_{net})} \quad (2)$$

The term q_{in} represents the specific input heat required per unit mass of the adsorbent. This specific energy input to the compressor is composed of several components: the specific heat of adsorption and the specific sensible heat contributions from the free gas within the compressor cell, the adsorbed gas, and the adsorbent material itself. These components can be expressed as follows:

$$q_{in} = q_{sorp.} + q_g + q_{g,ads} + q_{carb} \quad (3)$$

The *COP* of the JT cold stage (COP_{JTCS}) can be defined as the ratio of the cooling power to the minimum work necessary for compressing the working gas from an initial low pressure (P_L) to the required high pressure (P_H). This minimum work corresponds to the Gibbs free energy change (Δg). In the ideal case, where the inlet and outlet temperatures of the compressor are identical, the change in specific Gibbs free energy aligns with the specific exergy (e) of the sorption compressor [14] [18].

$$COP_{JTCS} = \frac{\dot{Q}_c}{\dot{m}_g \cdot e} = \frac{\Delta h_c}{\Delta g} \quad (4)$$

The cooling power at the cold tip (\dot{Q}_c) can be expressed as:

$$\dot{Q}_c = \dot{m}_g \cdot \Delta h_c \quad (5)$$

where Δh_c denotes the maximum achievable specific enthalpy difference between the high and low pressure gas lines, indicative of the maximum heat transfer that occurs across the coldest CFHX (the one connected to the JT expansion device), assuming 100% effectiveness. Meanwhile, the term \dot{m}_g corresponds to the mass-flow rate of the gas.

2.5.4. Step 2: optimization process

A range of operating settings (low and high pressures, and compressor high temperatures) is selected using the steady-state model, aiming to find the regions of maximum cooler's total COP (for each of the three stages). An acceptable optimum design range is first examined before converging to the precise value selection of the optimum operating conditions. As an illustration, such a range is indicated in Fig. 5 as a rectangle on the COP performance plot, with high pressure and compressor high temperature as the varied parameters. In the following paragraphs, the optimizations of the three stages are considered separately.

Helium Stage

The helium stage, which is the final cooling stage, is precooled by the hydrogen and neon stages. The cold finger temperature requirement of 8 K is above the critical temperature of helium (5.19 K). As a result, helium remains in its gaseous phase throughout the expansion process. The cooling in this stage is established by the sensible heat, as a temperature difference is created between the exit of the JT expansion device (which is less than 8 K) and the targeted cold finger temperature of 8 K. This contrasts with the neon and hydrogen stages, where cooling is achieved through latent heat due to the occurrence of liquefaction. The performance of the helium stage also impacts the cooling loads on the other two stages. Furthermore, the COP of the helium compressor is relatively low because of the poor adsorption capacity at the operating sink temperature (70 K). Three operating parameters were optimized, namely the operating pressure pair (P_H , P_L) and the high temperature of the sorption compressor (T_H). The optimization search resulted in an acceptable range of values of 7.35 to 7.7 bar and 14 to 14.5 bar, for the low and high pressures, respectively. Similarly, at these pressure pair values, the optimum high temperature of the sorption compressor (T_H) is found to be in the range of 105–110 K.

Hydrogen Stage

The hydrogen stage is dedicated to cooling the innermost radiation shield of the ETpathfinder cryostat and to pre-cooling the helium cold stage. Due to the targeted 15 K operating temperature of the hydrogen stage, the cold stage evaporator should be at a sub-atmospheric low pressure (P_L) of 0.129 bar. To establish satisfactory performance both at the compressor and the cold stage levels, a large pressure ratio (P_H/P_L) is required. Therefore, a two-stage sorption compressor is employed. In this case, the high temperatures of both compressor stages, as well as their high pressures, are searched via the optimization algorithm. The COP optimization revealed that the pressure ratios of the 1st and 2nd stages should be close and in the range of 10 to 16. In addition, a wide range of pressure and temperature combinations can produce similar performance levels, meaning that the optimum operating setting regions have smooth peaks (low variation of COP).

Neon Stage

The neon stage aims to cool the intermediate radiation shield and to pre-cool the helium and hydrogen cold stages at 40 K. The corresponding saturation pressure in the evaporator (i.e., the low pressure in the neon system) is 14.65 bar. The analysis revealed that rather elevated values are needed for the high pressure to produce a satisfactory performance (95–120 bar). We decided to select a value of 95.9 bar, akin to the high pressure of the neon stage in the METIS cooler [19]. This high-pressure value also determines the thickness of the container, which is consistent across all cells in the sorption cooler (see section 2.4). A single sorption compressor stage is used with no pre-cooling at the JT cold stage (other than heat sinking at the LN_2 shield, see Fig. 3).

Table 4

Sorption cooler stages optimized operating settings.

Sorption Cooler Stage	Pressures ($P_L P_H$) [bar]	High Temperature (T_H) [K]	Pre-cooling Temperatures & Heat Loads ($T_{Prec} Q_{Prec}$) [K mW]
Helium	14.11 – 7.7	107.1	40 – 35.1 15 – 65.6
Hydrogen (1 st)	1.91 – 0.129	128.4	40 – 454.3
Hydrogen (2 nd)	24.1 – 1.91	152.3	
Neon	95.9 – 14.65	150.5	-

Table 5

Reference operating settings for the model validation case.

Operating Parameter	Average T_{sink} [K]	P_H [bar]	P_L [bar]	t_{ht} [sec]	t_{cycle} [sec]	Q_{ht} [W]
Value	70	14.08	7.48	8.73	103.6	150

Based on the above remarks, the selected operating settings for each stage are detailed in Table 4. This table also presents the heat loads associated with the respective pre-cooling heat exchangers.

2.5.5. Step 3: dynamic model

A 1D dynamic thermo-adsorption model was developed to simulate the sorption cell dynamic behavior. According to the sorption cell design discussed in section 2.4, it is worth clarifying that the adsorbent-adsorbate design element is simulated as a mixture of activated carbon, gas in its adsorbed state and its free gaseous state. To compute the sorption cell temperature field, the heat balance equation that is presented below needs to be solved:

$$\underbrace{\rho c_p \frac{\partial T}{\partial t}}_{\text{energy content term}} = \underbrace{\nabla \cdot (\lambda \nabla T)}_{\text{conduction term}} + \underbrace{(\ddot{Q}_{ht} + \ddot{Q}_{h,flow} + \ddot{Q}_{sorp})}_{\text{heat source term}} \quad (6)$$

The finite volume approach is used for the spatial discretization of the sorption cell. The thermal energy in a finite volume (thermal node) can change as a consequence of conductive heat transfer with neighboring nodes and actively heating it with a heater (\ddot{Q}_{ht} , applied on the heater node), as shown in Eq. (6). Likewise, two additional heat sources are taken into account: the enthalpy flow ($\ddot{Q}_{h,flow}$) in or out of the adsorbent mixture volumes as gas flows in or out of these nodes, and the heat of ad-or desorption (\ddot{Q}_{sorp}). The formulation of these two heat contributions can be found in [24] and [25]. During the compression and decompression phases (see Fig. 1), the total amount of gas in the compressor cell remains constant. Thus, the amount of free gas in the cell can be evaluated by determining the difference between the fixed total amount of gas and the total amount that is ad-or desorbed. Next, based on the temperature distribution (temperature of all individual nodes) and the assumption that the pressure is uniform across the cell, the corresponding pressure in the cell can be determined. For the inflow and outflow phases, the cell pressure is assumed to be constant ($P(t) = P_L$ and $P(t) = P_H$, respectively) and the amount of working fluid in the cell is recomputed (gain or loss in mass). All thermal properties are considered temperature-dependent in the simulations.

Dynamic Model Validation

The dynamic model is validated against the experimental performance of the METIS compressor cell with helium as the working fluid. This cell is schematically depicted in Fig. 4, and the dimensions and materials are listed in Table 2. In the simulation, the cell is divided into 27 nodes (1 heater node, 20 adsorbent mixture nodes, 5 isolator nodes, and 1 container node). The operating settings corresponding to the experiments performed on cell 3 in [21] are listed in Table 5 and implemented into the model.

Table 6
Comparison of experimental data to model predictions.

Comparison Criteria	Experimental Results	Simulation Results	Difference
Compression phase (sec)	5.5	5.1	7.8%
Outflow phase (sec)	6.5	10.2	-36.2%
Decompression phase (sec)	21.5	23.3	-7.7%
Inflow phase (sec)	70.1	65	7.8%
Cycle mass flow rate [mg/s]	2.73	2.41	13.3%

The phases of the sorption cycle, as well as the delivered mass-flow rates observed in the experiments [21] and those obtained from the simulations, are outlined in Table 6. The single cell mass flow is underestimated by 13.3% in the model. From a system level perspective, the underestimation in the cell mass flow brings the model on the safe side of the design margins (conservative approach). The sorption cycle-phases are within a 10% difference except for the outflow phase duration that has a discrepancy of 36%, as the model predicts 10.2 sec versus the measured 6.5 sec. We suspect that the constant pressure modeling assumption during this phase, mainly accounts for this deviation. There will be a pressure gradient in axial direction as gas is pushed out at one end of the compressor cylinder (see Fig. 4). At this preliminary design phase we consider the deviations between model and experiments acceptable.

3. Discussion & results

This section presents the results of the performance analysis of the proposed sorption cryochain, detailed in section 3.1; A comparative study, investigating different cooler configurations relative to the proposed cryochain, is discussed in section 3.2; Additional design considerations concerning the operation of the proposed sorption cryochain are discussed in section 3.3.

3.1. ETpathfinder cooler baseline design: overall performance and size

The resulting overall sorption cooler system size and performance is presented. As pointed out in section 2.5.1 the selected operating conditions obtained by the thermodynamic evaluation are plugged into the sorption compressor cell dynamic model to estimate the delivered performance per cell. The achieved mass flow rate per compression cycle and the input powers are computed. Furthermore, the total number of required cells per cooler stage is evaluated. Considering the fact that the sorption compressor unit greatly determines the overall size of the entire sorption cryochain, the total number of cells is a good indication of that overall size. In the baseline design case the heat sink temperature of the sorption compressor is set to (T_{sink}) while the sink temperature of the cold stages is set to 77 K (see Fig. 3). Additionally, constant pulse heating of 150 W (\dot{Q}_{in}) is applied to each compressor cell. Table 7 summarizes the key results of the cryochain analysis. Note that in Table 7, $\dot{m}_{g,cell}$ indicates the mass flow rate generated per cell under these conditions. Similarly, $\dot{Q}_{in,cell}$ indicates the average power fed into a single cell, i.e. (t_{hi}/t_{cycle}) \times 150 W. The ratio ($\dot{m}_{g,tot}/\dot{m}_{g,cell}$) determines the required number of cells (N_{cells}), and this number is rounded up to the nearest integer. This results in an additional design margin. In Table 7, this margin is used to reduce the average required input power according to the following relation:

$$\dot{Q}_{in,tot} = \left(\frac{\dot{m}_{g,tot}}{\dot{m}_{g,cell}} \right) \dot{Q}_{in,cell} \quad (7)$$

Alternatively, one could prefer using the margin (at least partly) to increase cooling power in the separate stages. Thus the helium stage could gain 6%, the hydrogen stage 14%, and the neon stage 4% in cooling power. The schematic shown in Fig. 6 provides a concise overview of the ETpathfinder sorption cryochain baseline design. The baseline results are also mapped onto the cryochain diagram, to provide the key

system level quantities in more detail. In the baseline design, the cryochain comprises 26 sorption cells, amounting to an estimated sorption compressor unit volume of approximately 47 L,¹ and requires a total input power of 364.4 W.

3.2. Trade-off study of the proposed cryochain

During the design process of the sorption-based cooler chain, a trade-off study was undertaken to assess the performance of various potential cryochain configurations. The proposed baseline cryochain, comprising neon at 40 K, hydrogen at 15 K, and helium at 8 K, emerged as the optimal choice due to its superior thermal performance (in terms of COP) and fewer required compressor cells.

Simpler two-stage cryochain configurations, specifically those involving supercritical hydrogen/helium and neon/helium combinations, were also evaluated. These configurations have only two cooling stage temperatures. The optimized configurations featured intermediate stages at 34 K for supercritical hydrogen and 31 K for neon. They also included the 8 K cooling interface at the helium-stage cold tip. Both configurations handled a cooling load of 3 W at these intermediate stages. Although apparently simpler, the overall efficiencies of these alternative configurations were much lower, resulting in a significantly larger required number of cells: 44 cells for the hydrogen/helium configuration and 39 cells for the neon/helium configuration, compared to 26 cells in our baseline design, see Table 7.

This higher precooling temperature of the helium stage significantly impacts the COP and has been identified as a key factor influencing the design of the cryochain. To address this, the proposed baseline cryochain incorporates three different temperature levels, which not only reduces the radiative environment but also provides a significantly lower precooling temperature for the helium stage. Specifically, the helium stage benefits from two precooling stages at 40 K and 15 K, with the 15 K stage being the most significant. This approach improves the COP of the helium stage and creates a more favorable radiative environment, which is crucial for reducing radiative losses. This is a key factor in achieving the high effectiveness (99.5%) required for the coldest helium-stage CFHX. This trade-off study underscores the suitability of the proposed baseline cryochain, offering an optimal balance between COP and complexity.

Another alternative that could be considered is the use of a cryogen (helium) to achieve the operational mirror temperature of 10 K (or even below) in the ETpathfinder cryostat. However, this approach is not economically viable. Our current cooler design, which transfers a heat load of 2.5 W from the LN_2 thermal shield to the 40 K stage, would without actively cooled shields, lead to a helium boil-off rate of roughly 4 liters/h. Given a vessel size of around 100 liters, this would necessitate daily refills. With two mirror towers operating at 10 K, the daily requirement would be approximately 200 liters. If supplied by liquid helium, this would result in a significant cryogen consumption. These are rough estimates but, they underscore the excessive resource usage, rendering this approach impractical, the more since the Einstein Telescope will be 200 to 300 m underground. Furthermore, while the boil-off rate can be reduced by actively cooling shields, it's important to note that standard cryogenic coolers generate mechanical noise. Therefore, we have chosen our current design to balance the requirements of cooling efficiency and noise reduction, without the need for frequent helium refills.

3.3. Further design considerations

The proposed baseline ETpathfinder operational cryogenic cooling system, contains a number of design parameters that have an effect on

¹ Calculated as 39 L for total cell volume (26 x 1.5 L) plus an additional 20% for buffers, piping, and check valves.

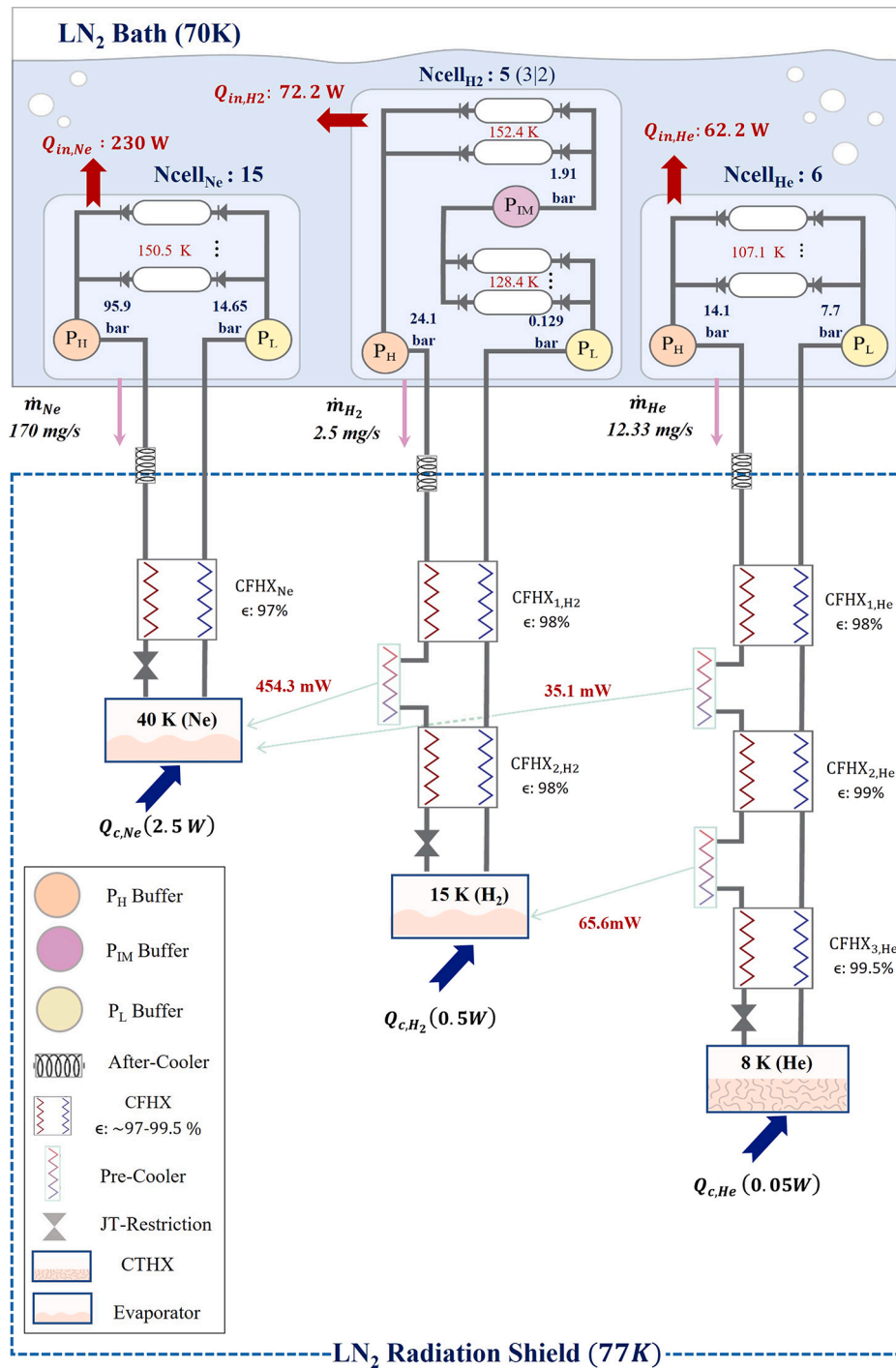


Fig. 6. ETpathfinder cryochain baseline design - Composed by 3 cooler stages (He 8 K - H₂ 15 K - Ne 40 K).

Table 7

Overall results of the sorption cooler baseline design.

Cooler Stage	Specifications		Operating Settings				Performance						
	\dot{Q}_c [W]	T_c [K]	P_H [bar]	P_L [bar]	T_H [K]	t_{ht} [sec]	$\dot{m}_{g,tot}$ [mg/s]	$\dot{m}_{g,cell}^a$ [mg/s]	t_{cycle} [sec]	$\dot{Q}_{in,cell}$ [W]	m_{curb} [g]	$\dot{Q}_{in,tot}$ [W]	N_{cell}
Helium	0.05	8	14.11	7.7	107.1	10.2	12.33	2.18	139.4	11	511	62.2	6
Hydrogen (1 st)	0.58 ^b	15	1.91	0.129	128.4	39.8	2.5	1.08	461.0	13.2	209	30.6	3
Hydrogen (2 nd)			24.1	1.91	152.4	77.4		1.43	500.8	23.8	158	41.6	2
Neon	3.09 ^b	40	95.9	14.65	150.5	82.4	170	11.76	775.4	15.9	1308	230	15
Total											2186	364.4	26

^a This value indicates the cell flow capacity as the outflow working gas flown out of the compressor divided by the cycle time.

^b Values include the pre-cooling loads and design margins (see Table 3).

the overall performance. We examined the sensitivity of design parameters, including the CFHX efficiencies, the cooling load at the helium-stage cold tip, the heat-sink temperature of the compressor, and the hydrogen evaporator saturation pressure. This section summarizes the results of this sensitivity analysis.

The efficiencies of the CFHXs and especially those of the coldest CFHX (prior to the gas expansion) greatly affect the performance of the cooler chain. The last CFHX of the helium stage can cause an increase up to 56% and 33% in required mass flow rate and input power, respectively, when deviating from the ideal 100% case to the 97% case. For the neon stage CFHX a drop of 10% in efficiency results in about 13% higher required mass flow rate. Furthermore, the required mass flow of the helium stage scales linearly with the cooling load at the cold tip (baseline value of $\dot{Q}_{c,He} = 0.05 \text{ W}$). In this case it is worth noting, at the higher helium flow rate, the precooling loads at the neon and hydrogen stages are also affected.

The sink temperature of the sorption compressor plays a crucial role in the performance of the entire cryochain. The sink temperature is varied from 80 K to 64 K. The helium compressor delivered mass flow then changes from 1.39 mg/s at $T_{sink} = 80 \text{ K}$ to 2.72 mg/s at $T_{sink} = 64 \text{ K}$, roughly doubled. Similarly, the number of cells and input power for the neon stage decreased by $\sim 29\%$ and $\sim 60\%$, respectively. The hydrogen stage was found to be the least affected by changes in the heat-sink temperature. The total number of cells decreased from 6 to 5, while the required input power declined by 34%.

In the baseline design the hydrogen cold tip temperature is set to 15 K which corresponds to an evaporator pressure that is well below atmospheric pressure (0.129 bar). Such a low evaporator pressure can potentially cause difficulties in managing the pressure level (pressure drops in connecting lines may become problematic), and the JT restriction could experience flow instabilities. For this reason we investigated the impact on the performance of the cryochain for hydrogen evaporator pressures of 0.32 bar ($T_{c,H_2} = 17 \text{ K}$) and 0.91 bar ($T_{c,H_2} = 20 \text{ K}$). For a hydrogen cold-tip temperature of 17 K the total input power increased marginally, with respect to the baseline value, by 1 W while one additional sorption cell is required (from 26 to 27 cells). Similarly, for a saturation pressure of 0.91 bar ($T_{c,H_2} = 20 \text{ K}$) the cryochain requires 386 W and 29 sorption cells.

4. Conclusion

In this paper, we introduce a conceptual design for a sorption-based cryochain that meets the cooling requirements of the ETpathfinder cryostat, which are 0.05 W at 8 K, 0.5 W at 15 K, and 2.5 W at 40 K. The baseline design of the cryochain consists of three thermally interconnected stages via pre-cooling stations. Each of these stages employs a sorption-based JT cooler, operating at respective temperatures of 8 K (helium stage), 15 K (hydrogen stage), and 40 K (neon stage). The compressors of these JT coolers are thermally driven and the absence of mechanically moving parts results in an absolute minimum of generated vibrations. We established a simulation workflow that uses a quasi-static thermodynamic model coupled with a dynamic sorption cell model. This hybrid workflow enabled an efficient optimization search for the operating settings of each stage (quasi-static model), followed by the performance evaluation, number of sorption cells and input power, per cooler stage (dynamic model). More precisely, the helium stage operates with relatively low pressure ratios since the working fluid is in its supercritical phase during the cooling process. In contrast, the hydrogen stage necessitates operating with high pressure ratios up to 186, given that its evaporator pressure is merely 0.129 bar. A 2-stage compression process is needed to efficiently establish such a high pressure ratio. As a result of the required 40 K evaporator temperature, the neon stage operates at a relatively high pressure at the evaporator (14.65 bar) which results in an elevated value of the system high pressure as well: 95.9 bar. The dynamic model is presented and is successfully validated against the experimental results of the METIS sorption cells.

These compressor cells are 0.5 m long and have an outer diameter of about 20 mm depending on the inside pressure (that determines the container wall thickness). Each cell contains 90.4 grams of Saran carbon. The baseline design performance results in 26 sorption cells with an estimated compressor unit volume of 47 liters and total input power of 364 W. Moreover, we conducted a trade-off study to evaluate the performance of two additional two-stage sorption cooler configuration ($H_2 : 34 \text{ K}/He : 8 \text{ K}$ and $Ne : 31 \text{ K}/He : 8 \text{ K}$). The alternative of using cryogen (helium) to achieve the required 10 K operating temperature of the mirrors is also discussed and concluded that is logistically impractical for the current application. The proposed baseline cryochain design ($Ne : 40 \text{ K}/H_2 : 15 \text{ K}/He : 8 \text{ K}$) emerged as the most suitable choice due to its superior thermal performance and the reduced complexity it offers in terms of the number of compressor cells required.

In order to further explore the design robustness of the proposed sorption-based cryochain a sensitivity analysis is performed studying various key system parameters: the efficiencies of counter flow heat exchangers (CFHXs), compressor heat-sink temperature and hydrogen-stage cold-tip temperature. The analysis demonstrated that the helium stage is highly sensitive to the efficiency of the coldest CFHX. A deviation of just 3% from the ideal case (100% efficiency) can lead to a 33% increase in required input power. Hence, in subsequent design phases, it is crucial to target an efficiency of over 99% for this CFHX. The compressor heat-sink temperature is a critical design parameter, as it can significantly impact the entire cryochain. Compared to the baseline design (70 K), a heat-sink temperature of 64 K can result in a reduction of over 20% in both overall input power and compressor size. In contrast, an 80 K sink temperature leads to a 33% and 44% increase in total size and input power, respectively. Interestingly, the hydrogen stage's cold-tip temperature has a relatively minor effect on the overall system performance. At 20 K, where the pressure was raised to 0.91 bar from 0.129 bar, the input power experienced a 6% increase, amounting to a total of 386 W. Concurrently, the number of cells also increased to a total of 29.

As future steps, we plan to revisit the sorption compressor cell design, which is now based on the previous METIS cooler system, such as to improve its performance tailored to the constraints and requirements of the ETpathfinder cryostat. Apart from the design also the heating pulse is to be optimized. Moreover, the vibration performance of the sorption coolers is of great importance and vibration studies are planned to be incorporated in the cryochain design evaluation. Next, a neon-stage compressor-cell module is aimed to be produced and tested.

Declaration of competing interest

The authors declare that they have no known competing financial interests or personal relationships that could have appeared to influence the work reported in this paper.

Data availability

Data will be made available on request.

Acknowledgement

This research is sponsored by Nikhef (through NWO-I) and the University of Maastricht (through EU Interreg).

References

- [1] Maggiore M, Broeck CVD, Bartolo N, Belgacem E, Bertacca D, Bizouard MA, et al. Science case for the Einstein telescope. *J Cosmol Astropart Phys* 2020;2020(03):050. <https://doi.org/10.1088/1475-7516/2020/03/050>.
- [2] ET Collaboration. ET design report update 2020. arXiv:ET-0007B-20. <https://www.et-gw.eu/index.php/relevant-et-documents>, 2020.
- [3] Hild S, Chelkowski S, Freise A, Franc J, Morgado N, Flaminio R, et al. A xylophone configuration for a third-generation gravitational wave detector. *Class*

- Quantum Gravity 2009;27(1):015003. <https://doi.org/10.1088/0264-9381/27/1/015003>. <https://dx.doi.org/10.1088/0264-9381/27/1/015003>.
- [4] The ETPathfinder Team. ETPathfinder design report. Available from: www.ETPathfinder.eu/research/.
- [5] Utina AC, Amato A, Arends J, Arina C, de Baar M, Baars M, et al. ETPathfinder: a cryogenic testbed for interferometric gravitational-wave detectors. *Class Quantum Gravity* 2022. <https://doi.org/10.1088/1361-6382/ac8fdb>.
- [6] The European Strategy Forum on Research Infrastructures. ESFRI announces new RIs for Roadmap 2021. Available from: www.esfri.eu/latest-esfri-news/new-ris-roadmap-2021/ [Accessed September 2022].
- [7] Aasi J, Abbott B, Abbott R, Abbott T, Abernathy M, Ackley K, et al. *Advanced ligo*. *Class Quantum Gravity* 2015;32(7):074001.
- [8] a. Acernese F, Agathos M, Agatsuma K, Aisa D, Allemandou N, Allocca A, et al. *Advanced Virgo: a second-generation interferometric gravitational wave detector*. *Class Quantum Gravity* 2014;32(2):024001.
- [9] Abe H, Akutsu T, Ando M, Araya A, Aritomi N, Asada H, et al. *The current status and future prospects of Kagra, the large-scale cryogenic gravitational wave telescope built in the Kamioka underground*. *Galaxies* 2022;10(3):63.
- [10] Nikhef, NWO-I. The Einstein telescope (Dutch web page). Available from: www.einsteintelelescope.nl/en/einstein-telescope/ [Accessed September 2022].
- [11] van Barneveld J, Saes L, Oomens I, van der Veen G. *Technopolis report: impact assessment of the Einstein Telescope*. <https://www.einsteintelelescope.nl/wp-content/uploads/2019/02/impact-assessment-of-the-einstein-telescope.pdf>, 2018.
- [12] Sakakibara Y, Akutsu T, Chen D, Khalaidovski A, Kimura N, Koike S, et al. *Progress on the cryogenic system for the Kagra cryogenic interferometric gravitational wave telescope*. *Class Quantum Gravity* 2014;31:224003. <https://doi.org/10.1088/0264-9381/31/22/224003>.
- [13] Caparrelli S, Majorana E, Moscatelli V, Pascucci E, Perciballi M, Puppo P, et al. *Vibration-free cryostat for low-noise applications of a pulse tube cryocooler*. *Rev Sci Instrum* 2006;77:95102. <https://doi.org/10.1063/1.2349609>.
- [14] Wiegierinck GFM. *Improving sorption compressors for cryogenic cooling*; 2005.
- [15] Wiegierinck GFM, Burger JF, Holland HJ, Hondebrink E, ter Brake HJM, Rogalla H. *A sorption compressor with a single sorber bed for use with a Linde-Hampson cold stage*. *Cryogenics* 2006;46:9–20. <https://doi.org/10.1016/j.cryogenics.2005.08.006>.
- [16] Burger JF, ter Brake HJM, Holland HJ, Meijer RJ, Veenstra TT, Venhorst GCF, et al. *Long-life vibration-free 4.5 K sorption cooler for space applications*. *Rev Sci Instrum* 2007;78:65102. <https://doi.org/10.1063/1.2745245>.
- [17] Pearson D, Bowman R, Prina M, Wilson P. *The Planck sorption cooler: using metal hydrides to produce 20 K*. *J Alloys Compd* 2007;446–447:718–22. <https://doi.org/10.1016/j.jallcom.2006.11.202>.
- [18] Wu Y, Zalewski DR, Vermeer CH, ter Brake HJM. *Optimization of the working fluid for a sorption-based Joule-Thomson cooler*. *Cryogenics* 2013;58:5–13. <https://doi.org/10.1016/j.cryogenics.2013.07.007>.
- [19] Wu Y, Zalewski DR, Vermeer CH, Holland HJ, Benthem B, ter Brake HJM. *Baseline design of a sorption-based Joule-Thomson cooler chain for the Metis instrument in the e-elt*. *Cryogenics* 2017;84:37–52. <https://doi.org/10.1016/j.cryogenics.2017.04.003>.
- [20] Wu Y, Vermeer CH, Holland HJ, Benthem B, ter Brake HJM. *Development of a switchless sorption compressor for the cryogenic refrigeration within the Metis instrument: part I. Theoretical design*. *Int J Refrig* 2017;82:520–8. <https://doi.org/10.1016/j.ijrefrig.2017.06.029>.
- [21] Wu Y, Vermeer CH, Holland HJ, Benthem B, ter Brake HJM. *Development of a switchless sorption compressor for the cryogenic refrigeration within the Metis instrument: part ii. Experimental demonstration*. *Int J Refrig* 2017;82:529–40. <https://doi.org/10.1016/j.ijrefrig.2017.06.023>.
- [22] National Institute of Standards and Technology. *Cryogenic materials properties reference list*. <https://www.nist.gov/mml/acmd/cryogenic-materials-properties-reference-list>, 2022.
- [23] Box GE, Hunter WG, Hunter JS. *Statistics for experimenters: design, innovation, and discovery*. 2nd edition. Wiley; 2005.
- [24] Wu R. *Development of a sorption-based Joule-Thomson cooler for the Metis instrument on e-elt*. 11, 2015. <https://doi.org/10.3990/1.9789036539937>.
- [25] Wu Y, Mulder T, Vermeer CH, Holland HJ, ter Brake HJM. *A 1-dimensional dynamic model for a sorption-compressor cell*. *Int J Heat Mass Transf* 2017;107:213–24. <https://doi.org/10.1016/j.ijheatmasstransfer.2016.11.040>.